Structure, Vibrations, Molecular Orbitals, Reactivity Properties of 3-Trifluoromethylphenylchloroformate by FT-IR, FT-Raman, FT-NMR and DFT Studies

V. Arjunan[1,2,*,], S. Senthilkumari[1] and S. Mohan[3]

[1]Department of Chemistry, Kanchi Mamunivar Centre for Post-Graduate Studies, Puducherry-605008, India
[2]Rajiv Gandhi Arts & Science College, Thavalakuppam, Puducherry-605007, India
[3]Department of Physics, S.A. Engineering College, Chennai-600077, India

*Corresponding author: E-mail: varjunftir@yahoo.com

The geometry of 3-trifluoromethylphenylchloroformate (FMPCF) was optimized with B3LYP method using 6–311++G** and cc–pVTZ basis sets. The molecular structural parameters and thermodynamic properties of the compound have been determined. The vibrational frequencies of the fundamental modes of the compound have been precisely assigned, analyzed and the theoretical results were compared with the experimental data. The energies of important molecular orbitals of the compound are also evaluated from DFT method. The Frontier orbital energy gap (E_{LUMO}–E_{HOMO}) is found to be 6.2143 eV. The extreme limits of the electrostatic potential is $+8.301e \times 10^{-3}$ to $-8.301e \times 10^{-3}$ while the total electron density spreads between $+3.835e \times 10^{-2}$ to $-3.835e \times 10^{-2}$. ^{1}H NMR and ^{13}C NMR chemical shifts are measured and compared with their gauge independent atomic orbital (GIAO) calculated values. The n(O7) $\rightarrow$ π*(C13–O14) and π(C1–C6) $\rightarrow$ π*(C2–C3) transitions are best stablized with 48.40 and 21.03 kcal mol^{-1}, respectively. In 3-trifluoromethylphenylchloroformate, the atoms C13 is favourable for electrophilic attack. The atoms C2 and C8 are more favourable for nucleophilic attack. The dual descriptors (Δf_k, Δs_k and $\Delta \omega_k$) revealed that the order of nucleophilic attack is C1 > C4 > C2 > C8 > C5. Thus, the present investigation provides complete structure, vibrations and reactivity characteristics of the compound.

Keywords: 3-Trifluoromethylphenylchloroformate, Molecular orbitals, DFT, Spectal studies.

INTRODUCTION

Due to the high electronegativity and small size of fluorine, the replacement of hydrogen atoms by fluorine in organic compounds often results in the profound change in their physical and chemical properties, including the stability, high lipophilicity and bioavailability [1-3]. Organo fluorine compounds have found broad applications in both life science and material sciences. Around 20 % of all pharmaceuticals and 30–40 % of all agrochemicals on the market contain fluorine [4,5]. Nucleophilic and perfluoroalkylation using organometallic compounds of lithium, magnesium and zinc has been vastly studied [6]. Chloroformates are useful catalysts for the polymerization of unsaturated compounds and in the preparation of polycarbonates, polyesters and formaldehyde polymers. Chloroformates are used as intermediates in the synthesis of pesticides, herbicides, perfumes, pharmaceuticals, foods, polymers and dyes. Chloroformates are also used for conversion to peroxydicarbo-

nates, which then serve as free radical initiators for polymerization of vinyl chloride, ethylene and other unsaturated monomers. The preference for the *syn* conformation was recently found for 3–trifluoromethylphenylchloroformate $ClCO_2C_6H_4OCF_3$ [7]. The *syn* conformer of $ClCO_2C_6H_4OCF_3$ is more stable than the *anti* form by 1.0 kcal mol^{-1}.

In this investigation bond parameters, vibrational fundamental modes, chemical shifts, topology of charge distributions, Frontier molecular orbital energies and reactive sites of 3–trifluoromethylphenylchloroformate (FMPCF) are analyzed by combining theoretical DFT methods and FT–IR, FT–Raman and FT–NMR experimental techniques.

EXPERIMENTAL

The compound 3–trifluoromethylphenylchloroformate is purchased from Aldrich Chemicals, U.S.A and used as such to record FT–IR, FT–Raman and FT–NMR spectra. The FT–IR spectrum of the compound is recorded by KBr pellet method

in the region 4000–400 cm^{-1} using Bruker IFS 66V spectrometer with a Globar source, Ge/KBr beam splitter and a MCT detector. The FT–Raman spectrum are also recorded in the range 4000–100 cm^{-1} by the same instrument with FRA 106 Raman module equipped with Nd:YAG laser source with 200 mW powers operating at 1.064 μm. A liquid nitrogen cooled–Ge detector is used. The ^{1}H (400 MHz; CDCl$_3$) and ^{13}C (100 MHz; CDCl$_3$) nuclear magnetic resonance (NMR) spectra are recorded on a Bruker HC400 instrument. The chemical shifts for protons are reported in ppm scales (δ scale) downfield from tetramethylsilane.

Computational details: The optimized geometrical parameters, thermodynamic properties, the charges of the atoms and vibrational frequencies of the compound FMPCF are determined by gradient corrected density functional theory (DFT) [8] with the three–parameter hybrid functional (B3) [9,10] for the exchange part and the Lee–Yang–Parr (LYP) correlation functional [11] with high level cc–pVTZ and 6–311++G** basis sets using Gaussian–09 [12] program.

The molecular electrostatic potential (MEP) and electron density [13] are calculated using 6–311++G** basis set. The molecular electrostatic potential (MEP) at a point r in the space around a molecule (in atomic units) can be expressed as:

$$V(r) = \sum_A \frac{Z_A}{|\vec{R}_A - \vec{r}|} - \int \frac{\rho(\vec{r}')dr'}{|\vec{r}' - \vec{r}|}$$

where, Z_A is the charge on nucleus A, located at R_A and $\rho(r')$ is the electronic density function for the molecule. The first and second terms represent the contributions to the potential due to nuclei and electrons, respectively. V(r) is the resultant electric potential at each point r, which is the net electrostatic effect produced at the point r by both the electrons and nuclei of the molecule. GaussView 5.0.8 visualization program [14] has been utilized to construct the MEP surface and the shapes of Frontier molecular orbitals. The energies of the molecular orbitals and HOMO–LUMO energy gap have also been calculated by using 6–311++G** and cc–pVTZ basis sets.

The Raman scattering activities (S$_i$) are converted to relative Raman intensities (I$_i$) using the following relationship derived from the basic theory of Raman scattering [15].

$$I_i = \frac{f(\nu_o - \nu_i)^4 S_i}{\nu_i[1 - \exp(-hc\nu_i/kT)]}$$

where, ν_o is the laser exciting frequency (cm^{-1}). In this work the excitation wavenumber is used as $\nu_o = 9398.5$ cm^{-1}, which corresponds to the wavelength of 1.064 μm for Nd:YAG laser, ν_i is the vibrational wavenumber of the ith normal mode, h–Plank constant, c–velocity of light and k–Boltzmann constant, f is the suitably chosen normalization factor (10^{-38}) for all the peak intensities and T–temperature in Kelvin (298.15 K).

The gauge independent atomic orbital (GIAO) method is used to calculate the ^{1}H and ^{13}C NMR isotropic nuclear magnetic shielding constants with accuracy [16,17]. The isotropic chemical shifts (δ) with respect to tetramethylsilane (TMS) are calculated from isotropic shielding values by $\delta_{iso}(X) = \sigma_{TMS}(X) - \sigma_{iso}(X)$, where δ_{iso} – isotropic chemical shift and σ_{iso} – isotropic shielding constant.

The chemical hardness, chemical potential, softness, electrophilicity, nucleophilicity and the appropriate local reactivity quantities are determined by natural population analysis using finite difference approximation. The vertical ionization potential (I), electron affinity (A) and the electron populations were determined on the basis of B3LYP/cc–pVTZ method. The energy calculations of the N–electron species were done using restricted B3LYP method while the energies of the N–1 and N+1 electronic species were calculated using open shell restricted B3LYP method using the optimized geometry of the N–electron species obtained from B3LYP/aug–cc–pVTZ method.

The site–selectivity of a chemical system can be determined by using Fukui function [18-20] which can be interpreted either as the change of electron density ρ(r) at each point r when the total number of electrons is changed or as the sensitivity of chemical potential (μ) of a system to an external perturbation at a particular point r.

$$f(r) = \left(\frac{\partial \rho(r)}{\partial N}\right)_{v(r)} = \left(\frac{\partial \mu}{\partial v(r)}\right)_N$$

The local softness s(r) describes the sensitivity of the chemical potential of the system to the local external perturbation and is obtained by simply multiplying Fukui function f(r) with global softness S.

$$s(r) = \left(\frac{\partial \rho(r)}{\partial \mu}\right)_{v(r)}$$

$$s(r) = f(r)S$$

where, S is inversely related to global hardness (η) as S = 1/2η.

Using the finite difference approximation, the Fukui functions for studying the reactivity at the atomic level are defined as:

$$f_k^+(r) = q_k(N+1) - q_k(N) \text{ for nucleophilic attack}$$

$$f_k^-(r) = q_k(N) - q_k(N-1) \text{ for electrophilic attack}$$

$$f_k^o(r) = \frac{1}{2}(q_k(N+1) - q_k(N-1)) \text{ for free radical attack}$$

In these equations, q_k is the atomic charge (evaluated from the natural population analysis) at the kth atomic site in the neutral (N), anionic (N+1) or cationic (N–1) molecular species. The global electrophilicity is calculated by the equation $\omega = \mu^2/2\eta$. The electrophilicity (s_k^+/s_k^-) and nucleophilicity (s_k^-/s_k^+) at the atomic levels are also determined.

RESULTS AND DISCUSSION

Conformational analysis and structure properties: Conformational analysis of 3-trifluoromethylphenylchloroformate (FMPCF) is carried out using B3LYP/6–31G** method. The potential energy surface diagram is obtained by the rotation of the carbonyl group with the dihedral angle (C1–O7–C13–O14) is shown in Fig. 1 and the possible conformations of the compound are shown in the Fig. 2. The compound FMPCF has three different conformers. The stability of the stable conformer is in the order I > II > III. The conformer (I) is more stable by 2.89 kcal mol^{-1} than that of the conformer II. The dihedral angle C1–O7–C13–O14 = 0° in the conformer I while it is
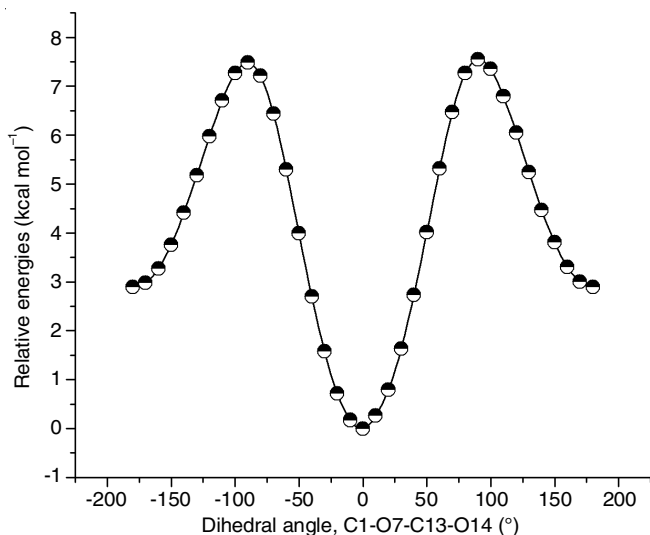
Fig. 1. Potential energy profile of 3–trifluoromethylphenylchloroformate

180° in conformer II. The carbonyl group does not lie in the plane of the ring and it is 40.3° tilted from the plane of phenyl ring. The energy difference between the conformer (II) and the third conformer (III) is 7.54 kcal mol⁻¹. In the conformer II the carbonyl group is tilted from the ring plane by an angle 92.8°. The dihedral angle C1–O7–C13–O14 of the third conformer is 90°. The conformer (III) corresponds to the transition state structure. In conformer III, the carbonyl group is tilted from the ring plane by 24.8°. The principal conformational difference between the two conformers I, II and III results from the orientation of the chloroformate and phenyl group. In all the conformers, the chloroformate moiety lie out of plane of the benzene ring while in II the chlorofomate moiety is orientated perpendicular to the benzene ring.

The optimized structural parameters, bond length and bond angle for the thermodynamically preferred geometry of FMPCF determined at B3LYP methods with 6–311++G** and cc–pVTZ basis sets are presented in Table-1 in accordance

with the scheme of numbering the atoms shown in Fig. 2. The calculated ring bond distances are very close to each other. Analyzing the bond angles of aromatic ring, one can observe that the geometry of the benzene ring is seen to be relatively perturbed due to the presence of substituents. The bond lengths and angles of the asymmetric unit of FMPCF are within normal ranges. In the structure of FMPCF the chloroformate (–OCOCl) moeity is perfectly planar. But it keeps out of planarity with the plane of the phenyl ring. The C=O carbonyl bonds (C4–O13) appear normal with lengths of 1.18 Å in relation to the carbonyl chloride bond at 1.1762 Å. The plane defined by the Cl–CO–O– group is rotated through dihedral angle of 180.0 to –180° relative to the adjacent phenyl ring. The phenyl ring is also planar. The dihedral angles C2–C1–O7–C13 and C6–C1–O7–C13 with 141.9° and 42.4°, respectively are most stable. The two O–C (ester) bond lengths are 1.34 Å (O7–C13) and 1.18 Å (C13–O14) confirm the presence of double bond between C13 and O14. The configuration and the C=O distance are similar to those observed in other chloroformate structures. The average C–C bond lengths of phenyl ring is 1.39 Å. In the phenyl ring both chloroformate and trifluoromethyl groups act as electron donating due to the high electonegativity of O7 and the three fluorine atoms in –CF₃ group. Thus, the bond angles at the *ortho* to the subsitituents (C1–C2–C3, C3–C4–C5 and C1–C6–C5) are less than 120°. The bond angle at point of substitution of trifluoromethyl group (C2–C3–C4) is more than 120°. Bond distances and angles in the FMPCF molecule compared well with values reported for other compounds containing a similar ring system. The C–F bond length is 1.35 Å. The CCF angle lie in the range 111.5 Å–112.2 Å and the FCF angles are found in the range 106.8–107.3°. All these data are well correlated with the experimental data [21,22].

Thermodynamic analysis: The total thermal energy, vibrational energy contribution to the total energy, the rotational constants and the dipole moment values obtained from B3LYP method with 6–31G(d,p), 6–311++G** and cc–PVTZ basis sets are presented in the Table-2. The energy of the com-
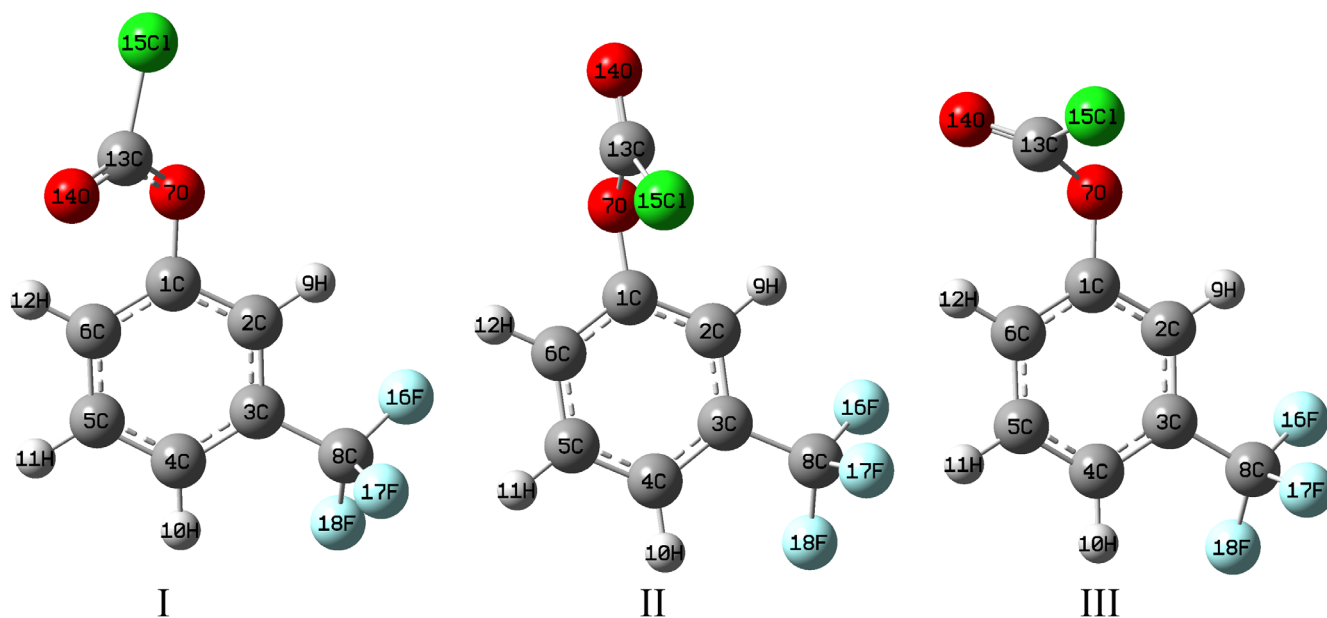
Fig. 2. Different conformers of 3–trifluoromethylphenylchloroformate

<div style="column: left">

TABLE-1
STRUCTURAL PARAMETERS OF
3–TRIFLUOROMETHYLPHENYLCHLOROFORMATE
DETERMINED BY B3LYP METHOD WITH
cc–pVTZ AND 6–311++G(d,p) BASIS SETS

Structural parameters	6–311++G(d,p)	cc–pVTZ	Expt.[a]
Internuclear distance (Å)			
C1–C2	1.39	1.38	1.366
C1–C6	1.39	1.38	1.377
C1–O7	1.41	1.41	1.424
C2–C3	1.39	1.39	1.378
C2–H9	1.08	1.08	0.930
C3–C4	1.40	1.39	1.380
C3–C8	1.51	1.51	0.930
C4–C5	1.39	1.39	1.366
C4–H10	1.08	1.08	0.930
C5–C6	1.39	1.39	1.387
C5–H11	1.08	1.08	0.930
C6–H12	1.08	1.08	0.930
O7–C13	1.34	1.34	1.310
C13–O14	1.18	1.18	1.177
C8–F16	1.36	1.35	
C8–F17	1.35	1.35	
C8–F18	1.35	1.35	
C13–Cl15	1.77	1.77	1.762
Bond angle (°)			
C2–C1–C6	122.1	122.0	122.0
C2–C1–O7	121.2	121.8	120.6
C6–C1–O7	116.5	116.1	117.1
C1–C2–C3	118.2	118.3	118.5
C1–C2–H9	120.9	121.0	120.7
C3–C2–H9	120.9	120.7	120.7
C2–C3–C4	120.9	120.8	120.2
C2–C3–C8	119.7	119.5	
C4–C3–C8	119.4	119.6	
C3–C4–C5	119.6	119.6	120.3
C3–C4–H10	120.0	119.9	119.9
C5–C4–H10	120.4	120.4	119.9
C4–C5–C6	120.3	120.3	120.3
C4–C5–H11	120.0	120.0	119.9
C6–C5–H11	119.7	119.7	119.9
C1–C6–C5	118.9	119.0	118.6
C1–C6–H12	119.6	119.5	120.7
C5–C6–H12	121.6	121.5	120.7
C1–C7–C13	118.8	119.4	116.5
C3–C8–F16	112.3	112.2	
C3–C8–F17	111.6	111.5	
C3–C8–F18	111.9	111.8	
F16–C8–F17	106.9	107.0	
F16–C8–F18	107.3	107.3	
F17–C8–F18	106.6	106.8	
O7–C13–O14	128.4	128.6	128.2
O7–C13–Cl15	108.0	107.8	107.2
O14–C13–Cl115	123.6	123.6	
Dihedral angle (°)			
O7–C1–C2–C3	175.8	175.7	–173.8
O7–C1–C6–C5	175.9	175.9	173.5
C2–C1–O7–C13	–58.6	–53.2	–61.1
C6–C1–O7–C13	125.8	131.2	124.8
C1–O7–C13–O14	0.1	0.1	–7.4
C1–O7–C13–Cl15	–179.8	–179.9	

[a]Values are taken from [Ref. 21,22]

</div>

<div style="column: right">

TABLE-2
THERMODYNAMIC PARAMETERS OF 3–
TRIFLUOROMETHYLPHENYLCHLOROFORMATE
DETERMINED BY B3LYP METHOD WITH
cc–pVTZ AND 6–311++G(d,p) BASIS SETS

Thermodynamic parameters (298 K)	cc–pVTZ	6–311++G(d,p)
SCF energy (a.u)	–1217. 7646935	–1217.6936499
Total energy (thermal), E_{total} (kcal mol^{-1})	76.225	75.948
Heat capacity at const. volume, C_v (cal mol^{-1} K^{-1})	43.175	43.398
Entropy, S (cal mol^{-1} K^{-1})	115.067	116.085
Vibrational energy, E_{vib} (kcal mol^{-1})	74.447	74.170
Zero–point vibrational Energy, E_0 (kcal mol^{-1})	68.711	68.389
Rotational constants (GHz)		
A	1.22	1.22
B	0.30	0.29
C	0.26	0.26
Dipole moment (Debye)		
μ_x	–0.07	0.16
μ_y	3.30	3.50
μ_z	–0.65	–0.72
μ_{total}	3.37	3.57
E_{LUMO+1} (eV)	–1.4052	–1.5873
E_{LUMO} (eV)	–1.5821	–1.7987
E_{HOMO} (eV)	–7.7964	–7.9627
E_{HOMO-1} (eV)	–8.0946	–8.2405
E_{LUMO} (eV) – E_{HOMO} (eV)	6.2143	6.1640
Ionization potential, I (eV)		0.4365
Electron affinity, A (eV)		–0.0705
Electronegativity (χ)		0.1830
Global hardness (η)		0.2535
Global softness (S)		1.9722
Chemical potential (μ)		–0.1830
Electrophilicity (ω)		0.0664

pound FMPCF determined by B3LYP/6–311++G** method is –1217.64135 Hatrees and for B3LYP/cc–PVTZ is –1217.71921 Hatress.

Analysis of molecular electrostatic potential: Molecular electrostatic potential (MEP) at a point in space around a molecule gives a visual understanding about the relative polarity of the molecule. The total electron density and MEP surfaces of the molecules under investigation are constructed by using B3LYP/6–311++G** method. The total electron density mapped with electrostatic potential surface, the contour map of electrostatic potential and molecular electrostatic potential surface of FMPCF are shown in Figs. 3-5. The colour scheme for the MEP surface is given as red: electron rich, partially negative charge; blue: electron deficient, partially positive charge; light blue: slightly electron deficient region; yellow: slightly electron rich region; green: neutral; respectively. Figs. 3 and 4 indicate that the region around oxygen atoms represents the most negative potential region (red). The total electron density of FMPCF lie in the range ± 3.835e × 10^{-2} while the extreme limits of the electrostatic potential is +8.301 × 10^{-3} and –8.301 × 10^{-3}.

Frontier molecular orbital analysis: The energy gap between highest occupied (HOMO) and the lowest unoccupied (LUMO) molecular orbitals has been used to prove the chemical reactivity and non–linear property. Hard and soft nucleophiles

</div>
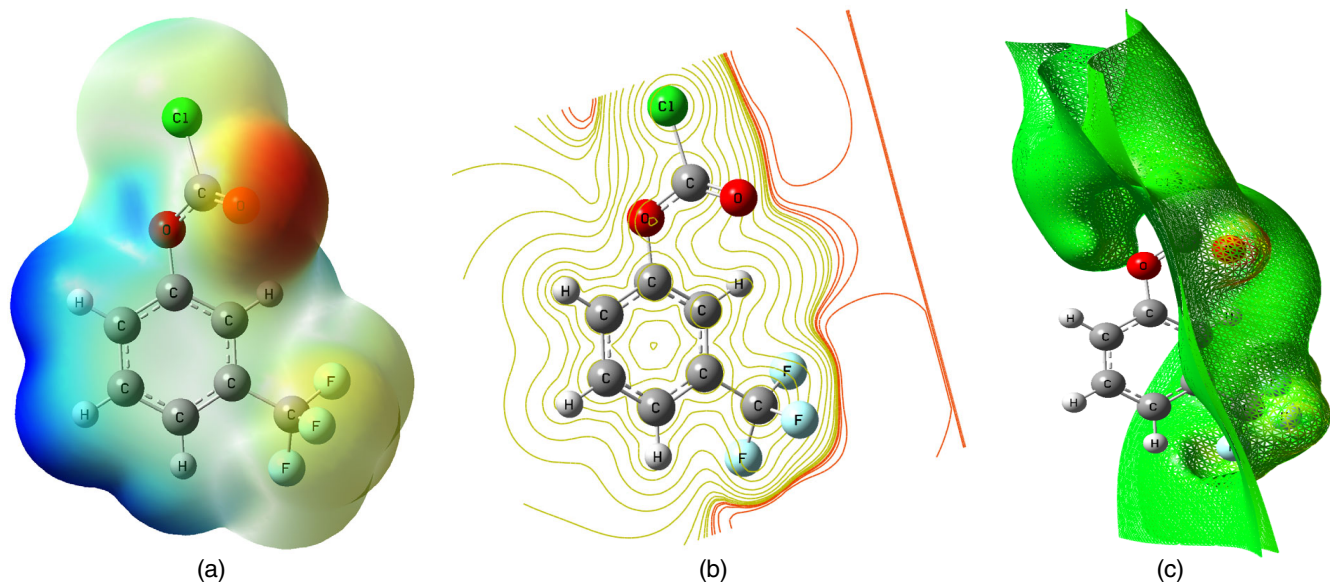
Fig. 3. (a) Total electron density surface mapped with electrostatic potential, (b) contour diagram of total electron density surface mapped with electrostatic potential and (c) electrostatic potential surface of 3–trifluoromethylphenylchloroformate
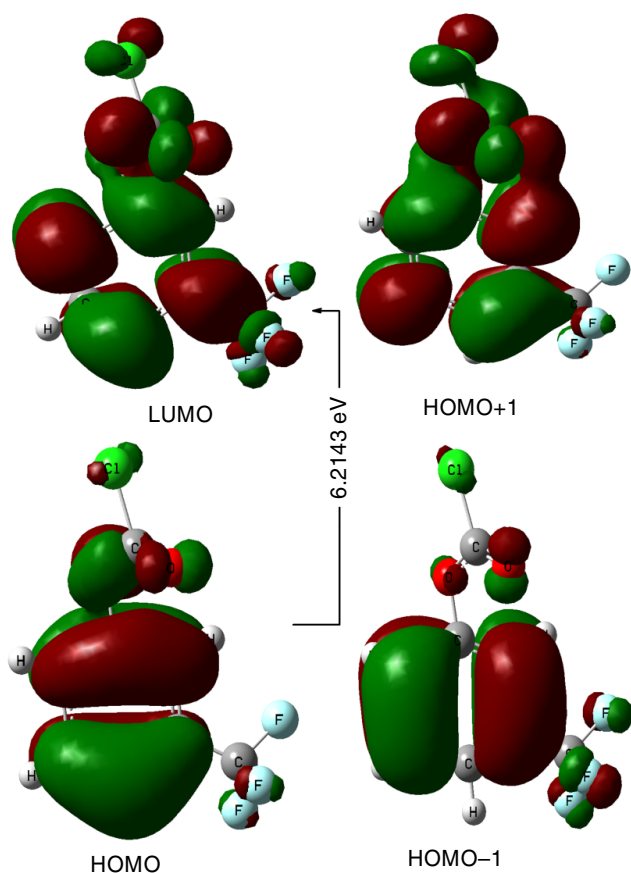
Fig. 4. Frontier molecular orbitals of 3–trifluoromethylphenylchloroformate

Fig. 5. FT–IR spectrum of 3–trifluoromethylphenylchloroformate

have a low and high energy HOMO, respectively while the hard and soft electrophiles have a high and low energy LUMO, respectively [23]. The HOMO energy is related to ionization potential and the LUMO energy is used to estimate the electron affinity and their average energy is related to electronegativity and the calculated LUMO–HOMO energy gap is closer to the first electronic excitation energy [24]. The Frontier orbital gap helps to characterize the chemical reactivity and kinetic stability

of the molecule. A molecule with a small Frontier orbital gap is more polarizable and is generally associated with a high chemical reactivity, low kinetic stability and is also termed as soft molecule [24]. The energies of HOMO LUMO, LUMO+1 and HOMO–1 and their orbital energy gaps are calculated by B3LYP/6–311++G** method and the pictorial illustration of their HOMO–LUMO distribution and their respective positive and negative region are shown in Fig. 4. The positive and negative phase is represented in red and green colour, respectively. The region of HOMO and LUMO levels spread over the entire molecule except the triflecomethyl group and the calculated energy gap of LUMO–HOMO is 6.2143 eV at B3LYP/cc–pVTZ method.

Natural bond orbital analysis: The atomic charges, atomic orbital occupancies and their parent and atomic hybrid contribution to atomic bonds and the delocalization of electron density, within the molecule are determined by natural bond orbital (NBO) analysis by B3LYP/6–311++G** method. The hybridization of the atoms and the weight of each atom in each localized electron pair bond is calculated in this idealized Lewis structure are determined. For FMPCF, no antibonding orbitals are listed

so that the structure is adequately explained by normal Lewis electron pair orbitals.

The bonding orbital for C1–C2 with 1.9795 electrons has 50.10 % C1 character in a $sp^{1.60}$ hybrid and has 49.90 % C2 character in a $sp^{1.86}$ hybrid orbital of FMPCF. A bonding orbital for C3–C4 with 1.9769 electrons has 51.12 % C3 character in a $sp^{1.73}$ hybrid and has 48.88 % C4 character in a $sp^{1.84}$ hybrid orbital of the compound. The bonding orbital for O7–C13 with 1.9887 electrons has 67.49 % O7 character in a $sp^{2.34}$ hybrid and 32.51 % C13 character in a $sp^{2.02}$ hybrid orbital. The bonding orbital for C13–O14 with 1.9883 electrons has 34.81 % C13 character in a $sp^{1.58}$ hybrid and 65.19 % O14 character in a $sp^{1.42}$ hybrid orbital. The C–C bonds of the benzene ring possess more *p* character than *s* character.

Donor acceptor interactions: Perturbation theory energy analysis: The Fock matrix analysis yield different types of donor–acceptor interactions and their stabilization energy. Second order perturbation theory analysis of Fock matrix of FMPCF and using NBO analysis [25,26] are presented in Table-3. The lone pair donor orbital, $n(O7) \rightarrow \pi^*(C13–O14)$ give a strong stabilization with 48.40 kcal mol^{-1} than $n(O14) \rightarrow \sigma^*(O7–C13)$ with stabilization of 32.78 kcal mol^{-1}. The $\pi_{CC} \rightarrow \pi^*_{CC}$ stabilization energy of electrons present in the C2–C3 bonding orbital and the C1–C6 antibonding orbital give a stabilization of 20.59 kcal mol^{-1}. The $\pi_{CC} \rightarrow \pi^*_{CC}$ stabilization energy of electrons present in the C1–C6 bonding orbital and the antibonding C2–C3 antibonding orbital is determined to give a strong stabilization, 21.03 kcal mol^{-1} than the $\pi_{CC} \rightarrow \pi^*_{CC}$ stabilization energy of electrons present in the C1–C6 bonding orbital and the antibonding C4–C5 is determined to give a stabilization of 18.88 kcal mol^{-1}.

The atomic charges of the neutral, cationic and anionic species of FMPCF are calculated by NBO analysis using the B3LYP/6311++G(d,p) method. All the ring carbon atoms possess negative charges except C1. The positive charge if C1 is due to the electronegativity of O7. The more positive charge of C13 is due to the ionic nature of carbonyl group. The very high positive charge of C8 is due to the attachment of highly electronegative fluorine atoms to it.

Vibrational analysis: The observed FTIR and FT–Raman spectra of FMPCF are shown in Figs. 5 and 6. The observed FTIR and FT–Raman wave numbers along with the theoretical infrared and Raman frequencies (unscaled and scaled), their relative intensities and probable assignments are summarized in Table-4. The vibrational assignment of all the fundamental modes is also supported by GaussView molecular visualization program [14].
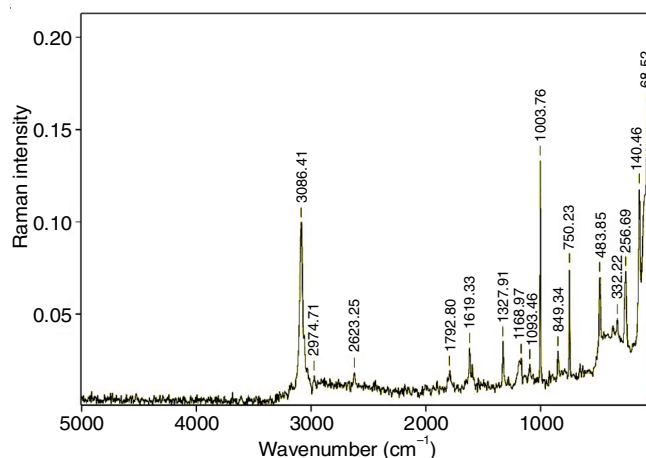
Fig. 6. FT–Raman spectrum of 3–trifluoromethylphenylchloroformate

C–H vibrations: The aromatic compounds show C–H stretching vibrations around 3100–3000 cm^{-1} range. In FMPCF these modes are observed at 3086, 3064 and 3037 cm^{-1}. The C–H in–plane bending vibrations are observed at 1086, 1030 and 979 cm^{-1} in FTIR and FT–Raman the in–plane bending vibration is observed at and 1093 cm^{-1}. The C–H out of plane bending modes [25,26], are usually medium intensity and attributed the FTIR bands observed at 919, 863 and 809 cm^{-1}.

Skeletal vibrations: The C=C bands mainly occur in the range of 1680–1640 cm^{-1}. The very strong to strong bands observed at 1591, 1555, 1441, 1391, 1343 cm^{-1} in FTIR spectrum are assigned to C–C stretching modes of FMPCF. The in–plane bending, trigonal bending mode is observed at 1004 cm^{-1} in FT–Raman and ring breathing mode is observed at 809 cm^{-1} in FTIR spectrum. The out of plane bending vibrations of the compound are observed in the low frequency region. The results are in good agreement with the literature values [27,28].

C=O vibrations: The C=O stretch lies in the spectral range 1750–1860 cm^{-1} and is very intense in the infrared and only moderately active in Raman. In FMPCF, the carbonyl stretching frequency is observed as a strong band at 1778 cm^{-1} in FTIR and in FT–Raman it is observed at 1793 cm^{-1}. The shifting in vibrational frequencies is higher due to the high electro negativity of chlorine atom attached to the carbonyl group. The inductive effect of chlorine attract electrons from

TABLE-3
SECOND ORDER PERTURBATION THEORY ANALYSIS OF FOCK MATRIX OF 3–TRIFLUOROMETHYLPHENYL CHLOROFORMATE BY NBO METHOD

Donor (i) → Acceptor (j)	E$^{(2)a}$ (kcal mol^{-1})	E(j) – E(i)^b (a.u.)	F(i, j)^e (a.u.)
π(C1–C6) → π*(C2–C3)	21.03	0.29	0.070
π(C1–C6) → π*(C4–C5)	18.88	0.30	0.067
π(C2–C3) → π*(C1–C6)	20.59	0.28	0.068
π(C2–C3) → π*(C4–C5)	20.24	0.29	0.069
π(C2–C3) → σ*(C8–F17)	6.09	0.52	0.053
π(C4–C5) → π*(C1–C6)	21.48	0.27	0.068
π(C4–C5) → π*(C2–C3)	21.63	0.28	0.069
n(O7) → π*(C13–O14)	48.40	0.33	0.115
n(O7) → π*(C1–C6)	9.17	0.37	0.054
n(O7) → σ*(C13–O14)	9.62	1.19	0.096
n(O14) → σ*(O7–C13)	32.78	0.61	0.130
n(O14) → σ*(C13–Cl15)	42.42	0.39	0.117
n(Cl15) → σ*(O7–C13)	5.63	0.65	0.055
n(Cl15) → σ*(C13–O14)	5.57	0.93	0.064
n(Cl15) → π*(C13–O14)	20.52	0.30	0.073
n(Fl6) → σ*(C8–F18)	11.02	0.68	0.078
n(Fl7) → σ*(C3–C8)	6.97	0.77	0.066
n(Fl7) → σ*(C8–F16)	10.13	0.67	0.074
n(Fl7) → σ*(C8–F18)	10.12	0.67	0.074
n(Fl8) → σ*(C8–F16)	10.95	0.68	0.077
n(Fl8) → σ*(C8–F17)	9.21	0.67	0.071

TABLE-4
OBSERVED FT–IR, FT–RAMAN AND CALCULATED FREQUENCIES USING B3LYP METHOD WITH
cc–pVTZ AND 6311++G(d,p) BASIS SETS ALONG WITH THEIR RELATIVE INTENSITIES AND
PROBABLE ASSIGNMENTS OF 3–TRIFLUOROMETHYLPHENYLCHLOROFORMATE

Observed wavenumbers (cm⁻¹)		Calculated wavenumber B3LYP/6–311++G(d,p)					Calculated wavenumbers B3LYP/cc–pVTZ					Vibrational assignments
FT-IR (KBr)	FT-Raman	Unscaled (cm⁻¹)	Scaled (cm⁻¹)	IR intensity	Raman intensity	Depolarization ratio	Unscaled (cm⁻¹)	Scaled (cm⁻¹)	IR intensity	Raman intensity	Depolarization ratio	
3365 m												2×1778
3297 m												2×1555
	3086 vs	3223	3094	2.78	0.16	0.22	3231	3102	2.38	0.25	0.26	νCH
3064 m		3209	3081	1.26	0.62	0.10	3211	3083	1.85	1.02	0.13	νCH
		3202	3074	0.51	0.18	0.74	3205	3076	0.85	0.35	0.59	νCH
3037 m		3187	3060	2.96	0.20	0.69	3188	3061	3.53	0.36	0.67	νCH
2912 m												2×1441
2858 m												2×1391
2635 m												2×1295
1778 s	1793 m	1855	1781	354.04	0.08	0.42	1855	1781	312.54	0.11	0.29	νC=O
1591 s	1619 m	1652	1586	1.44	0.32	0.72	1655	1589	1.61	0.46	0.72	νC=C
1555 s		1635	1570	17.13	0.20	0.71	1638	1572	18.53	0.33	0.66	νC=C
1441 m		1522	1461	16.55	0.01	0.75	1529	1468	17.98	0.01	0.69	νC=C
1391 s		1471	1412	68.32	0.03	0.75	1477	1418	66.19	0.04	0.73	νC–C
1343 m	1338 m	1352	1311	1.46	0.02	0.62	1355	1314	3.09	0.03	0.74	νC–C
1295 vs		1325	1285	195.61	0.24	0.10	1330	1290	189.73	0.36	0.11	ν_sCF$_3$
		1307	1268	171.68	0.29	0.08	1313	1274	166.14	0.40	0.09	νC–C
	1169 w	1200	1164	190.00	0.37	0.21	1205	1168	220.02	0.72	0.25	νC–O
		1187	1151	131.55	0.22	0.08	1191	1156	107.79	0.31	0.12	νC–CF$_3$
1131 vs		1155	1120	70.04	0.02	0.38	1174	1138	81.20	0.02	0.32	ν_aCF$_3$
1086 vs	1093 vw	1116	1083	521.06	0.10	0.75	1140	1106	264.73	0.14	0.62	βCH
		1111	1078	661.98	0.14	0.24	1120	1086	788.09	0.30	0.23	βCH
		1109	1076	6.04	0.09	0.56	1115	1082	31.22	0.11	0.75	νC–O
1030 vs		1079	1047	90.03	0.05	0.21	1086	1054	81.63	0.06	0.38	βCH
	1004 vs	1018	987	12.56	1.22	0.06	1024	993	11.47	1.82	0.08	βCCC (TB)
979 m		997	967	0.51	0.00	0.42	1006	976	1.02	0.01	0.73	βCH
919 vs		938	910	9.84	0.03	0.13	946	918	6.31	0.02	0.28	γCH
863 w		915	888	42.51	0.01	0.18	924	896	38.15	0.01	0.62	γCH
	849 w	889	862	25.07	0.02	0.71	893	866	19.61	0.04	0.67	βCCC (RB)
809 s		855	829	93.54	0.31	0.17	856	831	102.22	0.35	0.19	γCH
782 s		806	782	46.13	0.04	0.14	814	789	43.21	0.07	0.22	δ_sCF$_3$
746 vw	750 s	748	726	1.94	0.62	0.04	754	731	2.94	0.93	0.05	νC–Cl
692 w		706	685	25.91	0.01	0.13	715	693	24.01	0.02	0.35	βC=O
		681	661	10.66	0.01	0.73	685	664	10.21	0.02	0.65	γC=O
		664	644	21.31	0.08	0.73	668	648	19.79	0.15	0.68	γCH
		638	619	15.78	0.15	0.40	644	624	11.33	0.22	0.35	βCCC
582 m		593	575	20.92	0.02	0.25	595	577	21.67	0.03	0.33	δ_aCF$_3$
549 m		570	553	5.72	0.09	0.62	574	557	8.07	0.13	0.63	βCCC
		520	504	3.96	0.09	0.50	524	508	3.48	0.11	0.50	ρCF$_3$
475 w	484 vs	477	463	5.87	1.14	0.29	476	461	6.13	1.79	0.32	ωCF$_3$
		458	444	1.30	0.01	0.68	461	448	1.28	0.04	0.59	βC–O
		439	426	1.38	0.03	0.56	438	425	1.55	0.10	0.47	βC–O
		369	358	4.74	0.28	0.21	370	359	4.68	0.45	0.27	γC–O
	332 vw	338	328	4.00	0.10	0.58	340	330	3.85	0.17	0.60	γC–O
		322	312	4.29	0.29	0.59	323	313	3.87	0.44	0.63	βC–CF$_3$
	259 m	263	255	2.61	0.51	0.43	265	257	2.70	1.15	0.47	βC–Cl
		250	243	1.26	1.22	0.33	251	243	1.29	1.94	0.37	γCCC
		184	178	1.96	0.13	0.68	187	181	1.85	0.27	0.63	γC–Cl
	140 s	134	130	0.34	2.26	0.75	135	131	0.29	4.09	0.75	γC–CF$_3$
		81	81	0.53	3.60	0.61	82	80	0.41	6.11	0.65	γCCC
		53	53	0.10	5.92	0.73	55	53	0.11	10.08	0.73	γCCC
		18	18	0.56	100.00	0.71	23	23	0.54	100.00	0.70	γCCC
		17	17	0.22	6.18	0.70	19	19	0.14	28.71	0.75	γCCC

the C=O bond, which increases the force constant and leads to an increase in the absorption frequency [28,29].

CF$_3$ vibrations: The trifluoromethyl group has seven fundamentals frequencies, CF$_3$ group attached to an aromatic carbon absorbs strongly in the region 1360–1090 cm^{-1} [30]. In present case the strong modes of symmetric stretching vibration is absorbed at 1295 cm^{-1} in FTIR and asymmetric stretching vibration is assigned to 1131 cm^{-1}. In symmetric deformation (δ_sCF$_3$) mode is observed at 782 cm^{-1} and the asymmetric deformation (δ_aCF$_3$) is observed at 582 cm^{-1} in FTIR spectrum. All other vibrational modes of CF$_3$ group are presented in the Table-4 and these are in close agreement with the literature values [27,30].

C–Cl vibrations: The C–Cl stretching frequency is generally observed in the region 800–500 cm^{-1} which is depending on the configuration of the compound. The absorption bands arose at 746 and 750 cm^{-1} in FTIR and FT–Raman spectra, respectively are assigned to the C–Cl stretching vibration [31].

Scale factors: A better agreement between the computed and experimental frequencies can be obtained by using two scale factors [32-34]. Above 1400 cm^{-1} 0.96 and below this 0.97 are used to determine the scaled wavenumbers. The optimum scale factors minimize the residual.

$$\Delta = \sum_{i}^{N} \left(\lambda\omega_i^{Theor} - \nu_i^{Expt} \right)^2$$

where, ω_i^{Theor} and ν_i^{Expt} are the ith theoretical harmonic frequency and ith experimental fundamental frequency (cm^{-1}), respectively and N is the number of frequencies included in the optimization which leads to

$$RMS = \sqrt{\frac{\Delta}{N}}$$

The regression coefficients (R^2) are almost unity (0.9998) and the frequencies are much closer to the experimental values and thus more reliable. The determined RMS deviation for 6311++G** and cc–pVTZ basis sets are 11 and 12 cm^{-1}, respectively.

NMR spectral investigations: The gauge including atomic orbital [35-37] method is one of the most common approaches for calculating isotropic nuclear magnetic shielding tensors. The ^{13}C NMR and ^{1}H NMR chemical shifts calculations of the title compound has been carried out by GIAO method using B3LYP functional with cc–pVTZ basis set. The ^{1}H and ^{13}C theoretical and experimental chemical shifts, isotropic shielding constants (Table-5). The observed ^{1}H and ^{13}C NMR spectra of the compound in CDCl$_3$ solvent are given in the Figs. 7 and 8.

Unsaturated carbons normally display with chemical shift values from 100 to 200 ppm. The chemical shifts of all the aromatic carbon atoms lie in the range 117.91–149.34 ppm. The external magnetic field experienced by the carbon nuclei is affected by the electro negativity of the atoms attached to them. The effect of this is that the chemical shift of the carbon increases if the carbon is attached an atom like oxygen to it. The carbonyl carbon (C13) is assigned to the downfield signal at 151.31 ppm. The carbon atom C8 connected with the chloroformate group is assigned to the end of the chemical shift range at 132.33 ppm due to the high electronegativity of the fluorine
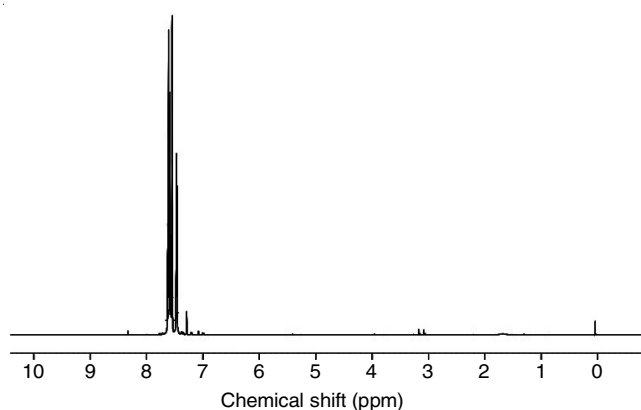
Fig. 7. ^{1}H NMR spectrum of 3–trifluoromethylphenylchloroformate
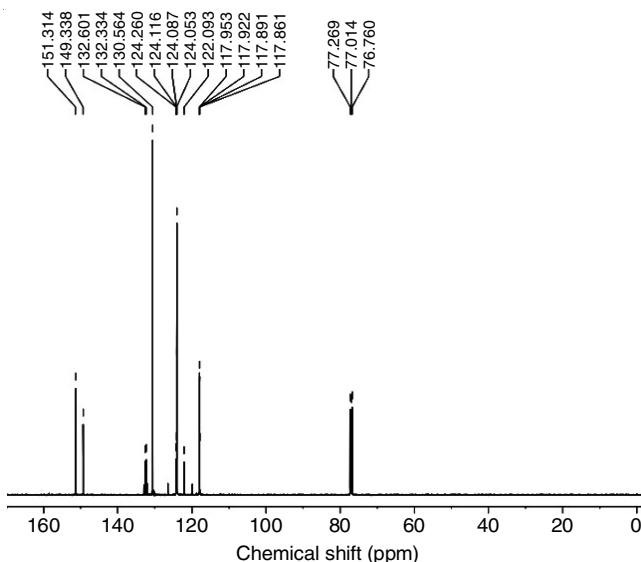
Fig. 8. ^{13}C NMR spectrum of 3–trifluoromethylphenylchloroformate

atoms. The more downfield chemical shift of C8 is due to the hyperconjugative effect of three fluorine atoms. The ^{13}C NMR chemical shifts determined theoretically are close agreement with the observed chemical shift.

The doublets observed at 7.46 ppm are assigned to the hydrogen atoms H10 and H12, respectively. The singlet observed at 7.29 ppm is attributed to H9. The H11 shows multiplets. The calculated and experimental chemical shift values are given in Table-5 shows good agreement with each other.

Analysis of structure–activity descriptors: Various reactivity and selectivity descriptors such as chemical hardness, chemical potential, softness, electrophilicity, nucleophilicity and the appropriate local quantities employing natural population analysis (NPA) are calculated. Both the global and local reactivity descriptors are determined using finite difference approximation to reveal the intramolecular reactivity of the molecule. The vertical ionization potential (I), electron affinity (A) and the electron populations are determined by B3LYP/6–311++G** method. The energy of the N–electron species is found by restricted B3LYP method while the energies of the N–1 and N+1 electronic species are calculated by using open shell restricted B3LYP method with 6–311++G** basis sets.

The atomic charges of neutral, cationic and anionic species of FMPCF was calculated by natural population analysis using

TABLE-5

EXPERIMENTAL AND CALCULATED ^{1}H NMR AND ^{13}C NMR ISOTROPIC CHEMICAL SHIFTS (δ_{iso}, ppm) WITH RESPECT TO TMS AND ISOTROPIC MAGNETIC SHIELDING TENSORS (σ_{iso}) OF 3–TRIFLUOROMETHYL PHENYLCHOLOROFORMATE

Assignment	σ_{iso} (^{1}H)	Cal. (δ_{iso})	Expt. (δ)	Assignment	σ_{iso} (^{13}C)	Cal. (δ_{iso})	Expt. (δ)
H9	23.82	8.15	7.29	C1	24.89	159.64	149.34
H10	23.82	8.15	7.46	C2	60.51	124.02	117.91
H11	23.86	8.11	7.59	C3	44.83	139.70	132.60
H12	24.16	7.81	7.46	C4	54.26	130.27	124.12
				C5	48.19	136.34	130.56
				C6	55.68	128.85	122.09
				C8	46.90	137.63	132.33
				C13	21.44	163.09	151.31

B3LYP/6–311++G** method are presented in Table-6. The understanding of chemical reactivity and site selectivity of the molecular systems have been effectively handled by the conceptual density functional theory [38]. Chemical potential, global hardness, global softness, electronegativity and electrophilicity are global reactivity descriptors, highly successful in predicting global chemical reactivity trends. The global parameters ionization potential (I), electron affinity (A), electrophilicity (ω), electronegativity (χ), hardness (η) and soft-ness (S) of the molecule are determined and displayed in Table-2.

The chemical potential measures the escaping tendency of an electron and it can be associated with the molecular electronegativity, while η determines the resistance of the chemical species to lose electrons and can be related to the stability and polarizability of the molecular system. On the other hand, the global electrophilicity index (ω) is defined as a measurement of the susceptibility of a chemical species to accept electrons.

Fukui function is a local reactivity descriptor that indicates the preferred regions where a chemical species will change its density when the number of electrons is modified. Therefore, it indicates the propensity of the electronic density to deform at a given position upon accepting or donating electrons.

Fukui functions play a prominent role that reflects the response of a molecular system towards a change in the number of electrons (N) of the molecular system under consideration. Fukui functions measure the response of the electron density at every point r, in front of a change in the number of electrons, under the constant external potential v(r) exerted by the nuclei. The sites with the largest value for the Fukui functions are those with the largest response and as such the most reactive sites within a molecule.

Fukui functions and local softness are extensively applied to probe the local reactivity and site selectivity. The formal definitions of all these descriptors and working equations for their computation have been described. The Fukui functions, local softness and multiphilicity descriptors of FMPCF calculated by B3LYP/6–311++G** method shows the Fukui functions represent the relative electrophilic and nucleophilic descriptors of FMPCF. The molecule under investigation mainly gives substitution reactions. In FMPCF, the atoms C13 is favourable for electrophilic attack. The atoms C2 and C8 are more favourable for nucleophilic attack. The dual descriptors (Δf_k, Δs_k and $\Delta \omega_k$) reveals that the order of nucleophilic attack is C1 > C4 > C2 > C8 > C5. The local softness, relative electrophilicity (s_k^+/s_k^-) and relative nucleophilicity (s_k^-/s_k^+) indices, the dual local softness Δs_k and the multiphilicity descriptors ($\Delta \omega_k$) have also been determined to predict the reactive sites of molecule and are summarized in Table-7.

Conclusion

A complete structural, thermodynamic, vibrational and electronic investigations along with FTIR, FT–Raman, FT–NMR and natural bond orbital analysis of FMPCF have been carried out with B3LYP method using large basis sets containing diffuse and polarization functions. Calculated data were compared with experimental results for infrared and Raman and all observed bands were assigned. The size, shape, charge distribution and site of high electro negativity of FMPCF has

TABLE-6

ATOMIC CHARGES AND FUKUI REACTIVITY DESCRIPTORS OF 3-(TRIFLUOROMETHYL)PHENYL CHLOROFORMATE DETERMINED BY NATURAL BOND ORBITAL ANALYSIS (NBO) USING B3LYP/6-311++G** METHOD

Atom	Neutral	Cation	Anion	f_k^+	f_k^-	f_k°	Δf_k
C1	0.2828	0.4721	0.2298	–0.0530	–0.1893	–0.1212	0.1362
C2	–0.2116	–0.1460	–0.2071	0.0045	–0.0656	–0.0306	0.0701
C3	–0.1216	–0.0887	–0.2525	–0.1309	–0.0329	–0.0819	–0.0980
C4	–0.1793	0.0456	–0.3025	–0.1232	–0.2249	–0.1741	0.1017
C5	–0.1754	–0.1431	–0.1842	–0.0088	–0.0323	–0.0206	0.0234
C6	–0.2120	–0.1516	–0.3998	–0.1879	–0.0604	–0.1241	–0.1275
O7	–0.4981	–0.4723	–0.5530	–0.0549	–0.0258	–0.0404	–0.0290
C8	1.0284	1.0590	1.0515	0.0231	–0.0306	–0.0037	0.0537
C13	0.7686	0.7291	0.6880	–0.0806	0.0395	–0.0206	–0.1201
O14	–0.5237	–0.4753	–0.5950	–0.0714	–0.0483	–0.0599	–0.0230
Cl15	–0.0523	0.0919	–0.1147	–0.0624	–0.1442	–0.1033	0.0818
F16	–0.3366	–0.3310	–0.3790	–0.0424	–0.0056	–0.0240	–0.0368
F17	–0.3350	–0.3231	–0.3860	–0.0510	–0.0119	–0.0315	–0.0392
F18	–0.3375	–0.3306	–0.3824	–0.0449	–0.0069	–0.0259	–0.0381

TABLE-7
LOCAL AND DUAL REACTIVITY DESCRIPTORS OF 3-(TRIFLUOROMETHYL)PHENYL
CHLOROFORMATE DETERMINED BY B3LYP/6-311++G** METHOD

Atom	s_k^+	s_k^-	s_k^0	Δs_k	ω_k^+	ω_k^-	ω_k^0	$\Delta\omega_k$	Electrophilicity	Nucleophilicity
C1	–0.0038	–0.0137	–0.0088	0.0099	–0.0953	–0.3402	–0.2177	0.2449	0.2802	3.5691
C2	0.0003	–0.0048	–0.0022	0.0051	0.0081	–0.1179	–0.0549	0.1260	–0.0686	–14.5778
C3	–0.0095	–0.0024	–0.0059	–0.0071	–0.2352	–0.0591	–0.1472	–0.1761	3.9772	0.2514
C4	–0.0089	–0.0163	–0.0126	0.0074	–0.2214	–0.4042	–0.3128	0.1828	0.5478	1.8255
C5	–0.0006	–0.0023	–0.0015	0.0017	–0.0159	–0.0580	–0.0369	0.0421	0.2736	3.6546
C6	–0.0136	–0.0044	–0.0090	–0.0092	–0.3376	–0.1085	–0.2230	–0.2291	3.1127	0.3213
O7	–0.0040	–0.0019	–0.0029	–0.0021	–0.0986	–0.0464	–0.0725	–0.0522	2.1243	0.4707
C8	0.0017	–0.0022	–0.0003	0.0039	0.0415	–0.0550	–0.0067	0.0965	–0.7549	–1.3247
C13	–0.0058	0.0029	–0.0015	–0.0087	–0.1448	0.0710	–0.0369	–0.2158	–2.0408	–0.4900
O14	–0.0052	–0.0035	–0.0043	–0.0017	–0.1282	–0.0869	–0.1076	–0.0413	1.4757	0.6776
Cl15	–0.0045	–0.0105	–0.0075	0.0059	–0.1122	–0.2591	–0.1857	0.1470	0.4328	2.3104
F16	–0.0031	–0.0004	–0.0017	–0.0027	–0.0762	–0.0100	–0.0431	–0.0662	7.5868	0.1318
F17	–0.0037	–0.0009	–0.0023	–0.0028	0.0164	–0.0213	–0.0024	0.0377	4.2991	0.2326
F18	–0.0033	–0.0005	–0.0019	–0.0028	0.0135	–0.0183	–0.0024	0.0317	6.5400	0.1529

been obtained by mapping electron density isosurface with molecular electrostatic potential. The extreme limits of the electrostatic potential is $+8.301e \times 10^{-3}$ to $–8.301e \times 10^{-3}$ while the total electron density spreads between $+3.835e \times 10^{-3}$ to $–3.835e \times 10^{-3}$. The ^1H and ^{13}C NMR chemical shifts are measured and compared with their GIAO calculated values. The Frontier orbital energy gap is found to be 6.2143 eV. The n(O7) → π*(C13–O14) and π(C1–C6) → π*(C2–C3) transitions are best stablized with 48.40 and 21.03 kcal mol^{-1}, respectively. In FMPCF, the atoms C_{13} is favourable for electrophilic attack. The atoms C_2 and C_8 are more favourable for nucleophilic attack. The dual descriptors (Δf_k, Δs_k and $\Delta\omega_k$) revealed that the order of nucleophilic attack is C1 > C4 > C2 > C8 > C5.

CONFLICT OF INTEREST

The authors declare that there is no conflict of interests regarding the publication of this article.

REFERENCES

1. K. Muller, C. Faeh and F. Diederich, *Science*, **317**, 1881 (2007); https://doi.org/10.1126/science.1131943.
2. J.P. Begue and D. Bonnet-Delpon, Sarcolemmal Cardiac KATP Channels as a Target for the Bioorganic and Medicinal Chemistry of Fluorine, Wiley: Hoboken, pp. 72–98 (2008).
3. W.K. Hagmann, *J. Med. Chem.* **51**, 4359 (2008); https://doi.org/10.1021/jm800219f.
4. P. Kirsch, N-Heterocyclic Carbenes in Transition Metal in Modern Fluoroorganic Chemistry: Synthesis, Reactivity and Applications. Wiley-VCH: Weinheim (2004).
5. R.E. Banks, B.E. Smart and J.C. Tatlow, Liquid Crystal, Materioal Design and sElf Assembly in Organofluorine Chemistry: Principles and Commercial Applications, Plenum: New York (1994).
6. G.K.S. Prakash and A.K. Yudin, *Chem. Rev.*, **97**, 757 (2007); https://doi.org/10.1021/cr9408991.
7. G.K.S. Prakash, F. Wang, T. Stewart, T. Mathew and G.A. Olah, *Proc. Natl. Acad. Sci. USA*, **106**, 4090 (2009); https://doi.org/10.1073/pnas.0900179106.
8. P. Hohenberg and W. Kohn, *Phys. Rev.*, **136**, 864 (1964); https://doi.org/10.1103/PhysRev.136.B864.
9. A.D. Becke, *J. Chem. Phys.*, **98**, 5648 (1993); https://doi.org/10.1063/1.464913.
10. A.D. Becke, *Phys. Rev. A*, **38**, 3098 (1988); https://doi.org/10.1103/PhysRevA.38.3098.
11. C. Lee, W. Yang and R.G. Parr, *Phys. Rev. B*, **37**, 785 (1988); https://doi.org/10.1103/PhysRevB.37.785.
12. M.J. Frisch, G.W. Trucks, H.B. Schlegel, G.E. Scuseria, M.A. Robb, J.R. Cheeseman, G. Scalmani, V. Barone, B. Mennucci, G.A. Petersson, H. Nakatsuji, M. Caricato, X. Li, H.P. Hratchian, A.F. Izmaylov, J. Bloino, G. Zheng, J.L. Sonnenberg, M. Hada, M. Ehara, K. Toyota, R. Fukuda, J. Hasegawa, M. Ishida, T. Nakajima, Y. Honda, O. Kitao, H. Nakai, T. Vreven, J.A. Montgomery Jr., J.E. Peralta, F. Ogliaro, M. Bearpark, J.J. Heyd, E. Brothers, K.N. Kudin, V.N. Staroverov, R. Kobayashi, J. Normand, K. Raghavachari, A. Rendell, J.C. Burant, S.S. Iyengar, J. Tomasi, M. Cossi, N. Rega, J.M. Millam, M. Klene, J.E. Knox, J.B. Cross, V. Bakken, C. Adamo, J. Jaramillo, R. Gomperts, R.E. Stratmann, O. Yazyev, A.J. Austin, R. Cammi, C. Pomelli, J.W. Ochterski, R.L. Martin, K. Morokuma, V.G. Zakrzewski, G.A. Voth, P. Salvador, J.J. Dannenberg, S. Dapprich, A.D. Daniels, O. Farkas, J.B. Foresman, J.V. Ortiz, J. Cioslowski and D.J. Fox, Gaussian 09, Gaussian, Inc., Wallingford CT (2009).
13. J.S. Murray and K. Sen, Molecular Electrostatic Potentials, Concepts and Applications, Elsevier: Amsterdam (1996).
14. R.I. Dennington, T. Keith and J. Millam, GaussView, Version 5.0.8, Semichem. Inc, Shawnee Mission, KS (2008).
15. G. Keresztury, S. Holly, G. Besenyei, J. Varga, A. Wang and J.R. Durig, *Spectrochim. Acta*, **49A**, 2007 (1993); https://doi.org/10.1016/S0584-8539(09)91012-1.
16. R. Ditchfield, *J. Chem. Phys.*, **56**, 5688 (1972); https://doi.org/10.1063/1.1677088.
17. K. Wolinski, J.F. Hinton and P. Pulay, *J. Am. Chem. Soc.*, **112**, 8251 (1990); https://doi.org/10.1021/ja00179a005.
18. R.G. Parr and W. Yang, *J. Am. Chem. Soc.*, **106**, 4049 (1984); https://doi.org/10.1021/ja00326a036.
19. W. Yang and R.G. Parr, *Proc. Natl. Acad. Sci. USA*, **82**, 6723 (1985); https://doi.org/10.1073/pnas.82.20.6723.
20. R.G. Parr and W. Yang, Density Functional Theory of Atoms and Molecules, Oxford University Press: Oxford (1989).
21. G.L. Bryant Jr. and J.A. King Jr., *Acta Crystallogr. C*, **50**, 1106 (1994); https://doi.org/10.1107/S0108270193011084.
22. S.-X. Bao, Z. Fang, Y.-L. Wang and P. Wei, *Acta Crystallogr. Sect. E Struct. Rep. Online*, **65**, o1606 (2009); https://doi.org/10.1107/S1600536809022600.
23. G. Klopman, *J. Am. Chem. Soc.*, **90**, 223 (1968); https://doi.org/10.1021/ja01004a002.
24. C.G. Zhan, J.A. Nichols and D.A. Dixon, *J. Phys. Chem. A*, **107**, 4184 (2003); https://doi.org/10.1021/jp0225774.
25. A.E. Reed and F. Weinhold, *J. Chem. Phys.*, **83**, 1736 (1985); https://doi.org/10.1063/1.449360.
26. A.E. Reed, R.B. Weinstock and F. Weinhold, *J. Chem. Phys.*, **83**, 735 (1985); https://doi.org/10.1063/1.449486.
27. V. Arjunan, L. Devi and S. Mohan, *J. Mol. Struct.*, **1159**, 103 (2018); https://doi.org/10.1016/j.molstruc.2018.01.049.

28. V. Arjunan, R. Anitha, S. Thenmozhi, M.K. Marchewka and S. Mohan, *J. Mol. Struct.*, **1113**, 42 (2016); https://doi.org/10.1016/j.molstruc.2016.02.034.

29. G. Varsanyi, Assignments for Vibrational Spectra of Seven Hundred Benzene Derivatives, vol. I, Adam Hilger: London (1974).

30. V. Arjunan, R. Anitha and S. Mohan, *Chem. Data Coll.*, **17–18**, 143 (2018); https://doi.org/10.1016/j.cdc.2018.08.006.

31. V. Arjunan and S. Mohan, *J. Mol. Struct.*, **892**, 289 (2008); https://doi.org/10.1016/j.molstruc.2008.05.053.

32. J.O. Jensen, A. Banerjee, C.N. Merrow, D. Zeroka and J. Michael Lochner, *J. Mol. Struct. THEOCHEM*, **531**, 323 (2000); https://doi.org/10.1016/S0166-1280(00)00465-6.

33. J.O. Jensen and D. Zeroka, *J. Mol. Struct. THEOCHEM*, **487**, 267 (1999); https://doi.org/10.1016/S0166-1280(99)00068-8.

34. H.F. Hameka and J.O. Jensen, *J. Mol. Struct. THEOCHEM*, **331**, 203 (1995); https://doi.org/10.1016/0166-1280(94)03888-R.

35. V. Arjunan, M. Kalaivani, S. Senthilkumari and S. Mohan, *Spectrochim. Acta*, **115**, 154 (2013); https://doi.org/10.1016/j.saa.2013.06.003.

36. H.O. Kalinowski, S. Berger and S. Braun, Carbon–13 NMR Spectroscopy, John Wiley & Sons: Chichester (1988).

37. K. Pihlaja and E. Kleinpeter, Carbon–13 Chemical Shifts in Structural and Sterochemical Analysis, VCH, Publishers: Deerfield Beach (1994).

38. P.W. Ayers and R.G. Parr, *J. Am. Chem. Soc.*, **122**, 2010 (2000); https://doi.org/10.1021/ja9924039.